

# Transient Stability Analysis with Physics-Informed Neural Networks

Jochen Stiasny, *Student Member, IEEE*, Georgios S. Misyris, *Student Member, IEEE*, Spyros Chatzivasileiadis, *Senior Member, IEEE*

**Abstract**—Solving the ordinary differential equations that govern the power system is an indispensable part in transient stability analysis. However, the traditionally applied methods either carry a significant computational burden, require model simplifications, or use overly conservative surrogate models. Neural networks can circumvent these limitations but are faced with high demands on the used datasets. Furthermore, they are agnostic to the underlying governing equations. Physics-informed neural network tackle this problem and we explore their advantages and challenges in this paper. We illustrate the findings on the Kundur two-area system and highlight possible pathways forward in developing this method further.

## I. INTRODUCTION

Analysing power system e.g. with respect to their transient behaviour is critical but difficult. The reliance on time-domain simulation incurs the burden of expensive evaluations which renders it impractical for screening or the evaluation of high-dimensional spaces. Derived simplified models, e.g. SIME [1], provide more opportunities with respect to screening actions but the drawbacks are related the continued use of time-domain simulations. Direct methods [2], [3] offer another fast method, it is usually linearised system and conservativeness that hinder a broad application. Machine learning and neural networks in particular might offer relief by providing a new approach and perspective at these problems as reviewed in [4]. However, they suffer from lacking trust on the side of grid operators due to the NN’s black-box nature and being agnostic to the well-studied physical models. That entails a enormous reliance on the datasets used for training and testing the models, yet the quality of the dataset can rarely be achieved from real-world datasets, be it because of insufficient dataset size, labelling or balancing. Hence, one needs to revert to simulations to provide the required datasets. Although the efficiency of these database generation has been improved [5], their high computational burden cannot be disregarded.

To counter this, attempts to incorporate the physical knowledge in form of the governing differential equations have been made. Such approaches [6] use the governing equations in the training process of a neural network, hereafter referred to as physics-informed neural network (PINNs). This allows to extend the perspective from a very dataset-focus process to a holistic approach that includes NN training, validation,

J. Stiasny, G. S. Misyris and S. Chatzivasileiadis are with the Technical University of Denmark, Department of Electrical Engineering, Kgs. Lyngby, Denmark (emails: [>{jbest, gmisy, spchatz}@elektro.dtu.dk](mailto:{jbest, gmisy, spchatz}@elektro.dtu.dk)).

This work is supported by Innovation Fund Denmark through the multiDC project (grant no. 6154-00020B).

and testing. The latter two, in particular, are key to build the missing trust of grid operators.

Following the initial approach in [7], our contributions relate to the extension of the method as follows:

- Improving the data efficiency of a dataset by including an additional loss term (dtNN)
- Tackling how to balance the multi-objective optimisation problem in the training process
- Performing a comparison between regular NNs and PINNs on the famous Kundur two-area system.
- Providing a publicly-hosted code base to foster adaption
- Providing the reader with an intuitive understanding

We begin by introduction the methodology in Section II and the case study to which we apply the method in Section III. In Section IV we extensively describe the inner workings of PINNs before pointing out opportunities and challenges associated with PINNs in Section V and closing in Section VI.

## II. METHODOLOGY

The governing equations of the transient stability problem in power systems are described by (1)-(2). Equation (1) collects the differential equations, which usually describe the generator and converter dynamics (and possibly the line dynamics if the focus is on the electromagnetic transients), while (2) collects the algebraic equations, which usually capture information about the network and the relationship between voltages, currents, and power flows [8]. Vector  $\mathbf{x}$  represents the dynamic states, which in their simplest form express the rotor angle and frequency of each generator at any time instant, and vector  $\mathbf{u}$  describes the system input, e.g. active power setpoints or disturbances.

$$\dot{\mathbf{x}} = \mathbf{f}(\mathbf{x}, \mathbf{u}) \quad (1)$$

$$\mathbf{0} = \mathbf{g}(\mathbf{x}, \mathbf{u}) \quad (2)$$

By specifying a pair  $(t_0, \mathbf{x}_0)$  which represents the initial conditions for our system, we can obtain a unique solution for (1)-(2) along time, that we call a *trajectory*. While the ODEs formulation, as shown in (1)-(2), yields a ‘nice’ form, a trajectory can not necessarily be represented in a closed form solution. Instead ODE solvers determine the trajectory by performing the integration numerically over small time steps. As this can be computationally expensive, we aim to find an explicit expression

$$\hat{\mathbf{x}}(t, \mathbf{x}_0, \mathbf{u}) \approx \mathbf{x}(t) \begin{cases} \frac{d}{dt} \mathbf{x} = \mathbf{f}(t, \mathbf{x}(t), \mathbf{u}) \\ \mathbf{x}(t_0 = 0) = \mathbf{x}_0 \end{cases} \quad (3)$$

that approximates the trajectory specified by the time instance  $t$ , the initial condition  $\mathbf{x}_0$  and the input variable  $\mathbf{u}$  across their input domain.

### A. Neural networks as function approximators

The following is based on the fact that neural networks can theoretically approximate any function [9], [10]. The practical limitation arises due to the limited representation capacity of the NN which is determined by its size, namely the number of hidden layers  $N_K$  and the number of neurons per layer  $N_L$ , as well as the non-linear activation function  $\phi$ . The NN that is subsequently used is formulated as

$$[t, \mathbf{x}_0, \mathbf{u}]^\top = \mathbf{z}_0 \quad (4)$$

$$\mathbf{z}_{k+1} = \phi(\mathbf{W}_{k+1}\mathbf{z}_k + \mathbf{b}_k) \quad \forall k = 0, 1, \dots, K-1 \quad (5)$$

$$\hat{\mathbf{x}} = \mathbf{W}_{K+1}\mathbf{z}_K + \mathbf{b}_{K+1}. \quad (6)$$

We fit the NN's parameters, the weights  $\mathbf{W}$  and biases  $\mathbf{b}$ , in a supervised fashion by minimising the loss  $\mathcal{L}_x^i$

$$\mathcal{L}_x^i = \frac{1}{N_x} \sum_{j=1}^{N_x} (x_j^i - \hat{x}_j^i)^2, \quad (7)$$

on each of the  $n$  states in  $\mathbf{x}$ , indicated by the superscript  $i$ . Each of the  $N_x$  data points, indexed by the subscript  $j$ , provides a mapping of the ground truth  $(t_j, \mathbf{x}_{0j}, \mathbf{u}_j) \rightarrow x_j^i$ . The training problem then formulates as

$$\min_{\mathbf{W}, \mathbf{b}} \sum_i \lambda_x^i \mathcal{L}_x^i \quad (8)$$

$$\text{s.t. (4) -- (6)} \quad (9)$$

where  $\lambda_x^i$  provides a weighing of the loss terms (see Section II-D).

Subsequently, we will keep the structure of the NN ((4)-(6)) but update the objective function (8) to achieve a better prediction accuracy. Figure 1 illustrates these different steps.

### B. Including physics at the data points - *dtNN*

In a first step towards more 'physical' interpolations, we enforce that the state update  $\mathbf{f}(t, \mathbf{x}(t), \mathbf{u})$  at the data points matches the temporal derivative of the NN's approximation  $\frac{d}{dt}\hat{\mathbf{x}}$ . We calculate  $\frac{d}{dt}\hat{\mathbf{x}}$  by applying automatic differentiation (AD) [11] on the NN's outputs  $\hat{\mathbf{x}}$  with respect to the input time  $t$ . This yields the loss terms  $\mathcal{L}_{dt}^i$

$$\mathcal{L}_{dt}^i = \frac{1}{N_x} \sum_{j=1}^{N_x} \left( f^i(t_j, \hat{x}_j, \mathbf{u}_j) - \frac{d}{dt} \hat{x}_j^i \right)^2 \quad (10)$$

which are then weighted and added to (8)

$$\min_{\mathbf{W}, \mathbf{b}} \sum_i \lambda_x^i \mathcal{L}_x^i + \sum_i \lambda_{dt}^i \mathcal{L}_{dt}^i \quad (11)$$

$$\text{s.t. (4) -- (6)} \quad (12)$$

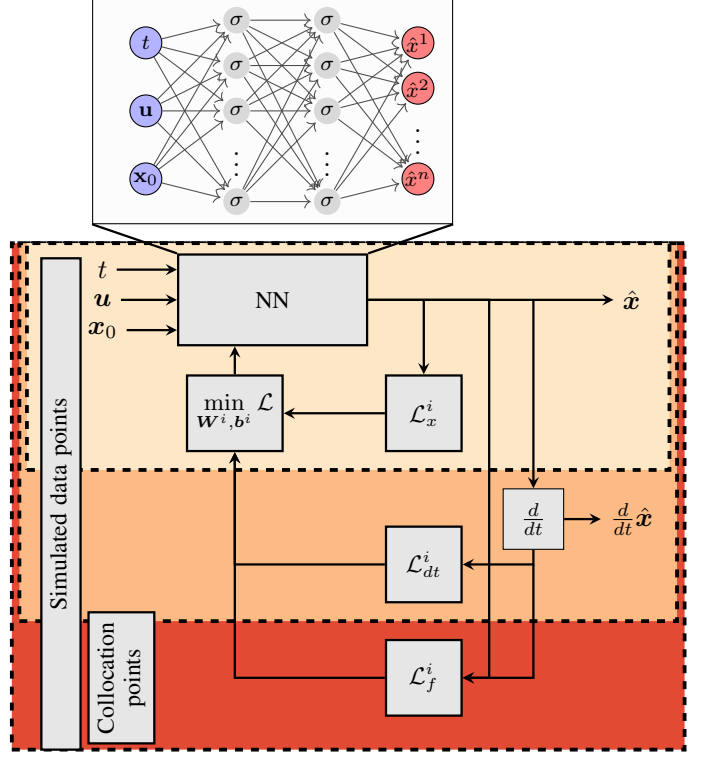


Figure 1. Structure of the different loss elements in the training procedure of PINNs displaying a simple NN (light orange), the incorporation of the derivative at data points (orange) and the additional of collocation points and the physical loss for PINNs (red).

### C. Probing physics at collocation points - *PINN*

The previous step of introducing *dtNNs* wrings out more information from the provided data points and their 'target values'  $\mathbf{x}_j$  than a simple NN. However, the quality of the NN's approximation is still purely dependent on the provided data points. PINNs in contrast use marginal information on the solution's accurateness without the need for knowing the true 'target value'  $\mathbf{x}_j$ . This works by comparing the state update based on the approximations  $f^i(t_j, \hat{x}_j, \mathbf{u}_j)$  and the derivative of the approximated state  $\frac{d}{dt}\hat{x}_j^i$ . The difference yields the loss term  $\mathcal{L}_f^i$

$$\mathcal{L}_f^i = \frac{1}{N_f} \sum_{j=1}^{N_f} \left( f^i(t_j, \hat{x}_j, \mathbf{u}_j) - \frac{d}{dt} \hat{x}_j^i \right)^2. \quad (13)$$

Since the calculation of  $\mathcal{L}_f^i$  does not require  $\mathbf{x}$ , we can evaluate  $\mathcal{L}_f^i$  at any point within the input domain, we refer to them as collocation points ( $N_f$ ). The training process is now updated once more to include  $\mathcal{L}_f^i$  weighted by  $\lambda_f^i$

$$\min_{\mathbf{W}, \mathbf{b}} \sum_i \lambda_x^i \mathcal{L}_x^i + \sum_i \lambda_{dt}^i \mathcal{L}_{dt}^i + \sum_i \lambda_f^i \mathcal{L}_f^i \quad (14)$$

$$\text{s.t. (4) -- (6).} \quad (15)$$

The intuition behind  $\mathcal{L}_f^i$  is as follows: We probe whether the prediction of the NN  $\hat{\mathbf{x}}$  and its derivative  $\frac{d}{dt}\hat{\mathbf{x}}$  are in themselves consistent with the governing equations. However, this does not necessarily mean that the prediction  $\hat{\mathbf{x}}$  is correct if  $\mathcal{L}_f^i = 0$ .

If, for example, the PINN outputs a constant value for  $\hat{x}$ , i.e.  $\frac{d}{dt}\hat{x} = 0$ , that exactly equals an equilibrium point, i.e.  $f(t, \hat{x}, u) = 0$ ,  $\mathcal{L}_f^i$  would equal 0 even if the desired trajectory is not the one of the equilibrium. Hence, training a PINN only by  $\mathcal{L}_f^i$  will not yield a satisfactory results. The lack of uniqueness can only be resolved if  $\mathcal{L}_x$  is included, though, in the spirit of the Picard-Lindelöf Theorem, a single value is sufficient to guarantee uniqueness provided that  $\mathcal{L}_f = 0$  along the entire trajectory. The initial condition  $x_0$  can fulfill this requirement and as we use  $x_0$  as an input rather than obtaining it as a result of a simulation, it is possible with PINNs to create the solution approximation  $\hat{x}$  without a single simulation.

#### D. Loss term weighing scheme

We require a single objective value for the machine learning optimisation algorithm, hence we weight the multiple loss terms in the total loss functions (8), (11), (14). The practical implications of balancing this multi-objective functions concern the accuracy and the training procedure. The reason being that each loss term shall have a similar influence on the adjustments of the NN's weights and biases. The computation of

$$\frac{d\mathcal{L}_x^i}{d(\mathbf{W}, \mathbf{b})}, \frac{d\mathcal{L}_{dt}^i}{d(\mathbf{W}, \mathbf{b})}, \frac{d\mathcal{L}_f^i}{d(\mathbf{W}, \mathbf{b})} \quad (16)$$

potentially yields distributions of different magnitudes. Without a weighing scheme a single loss term could guide the training while the other terms are largely ignored. To avoid such cases, that can lead to unfavourable local minima, we scale each loss term by the corresponding loss term weight  $\lambda_x^i$ ,  $\lambda_{dt}^i$ ,  $\lambda_f^i$ . The balancing of these terms is difficult and we rely as of now on a heuristic presented in Table I. The algorithm proposed by [12], is used as an indication how the loss term weights shall be chosen, however, a continuous update using the algorithm led to unsatisfactory results as its interference with the NN training algorithm created very imbalanced solutions. For the heuristic of Table I we therefore included the following considerations to adjust the outcome of algorithm:

- Equal weighing of like-wise states (generator rotor angles, generator frequency, load angles)
- Scaling of  $\lambda_x^i$ ,  $\lambda_{dt}^i$  according to the inter-quartile ranges across the dataset
- Adjusting  $\lambda_x^i$ ,  $\lambda_{dt}^i$  to account for the use of collocation points

Table I

LOSS TERMS WEIGHTS  $\lambda$  IN (8), (11), (14) WITH  $k = 2.2 \cdot 10^4 \cdot N_c/N$

	$\delta_1, \delta_2, \delta_3, \delta_4$	$\delta_5, \delta_6$	$\omega_1, \omega_2, \omega_3, \omega_4$
$\lambda_x$	$1.0 \cdot k$	$1.0 \cdot k$	$2.0 \cdot k$
$\lambda_{dt}$	$0.5 \cdot k$	$0.04 \cdot k$	$0.12 \cdot k$
$\lambda_c$	1000	3.0	5.0

### III. CASE STUDY - KUNDUR'S TWO-AREA SYSTEM

This section briefly presents a case on the Kundur two-area system which is well-known in the context of transient

stability analysis. We note that the case is mainly picked to highlight the fundamentals of PINNs rather than providing insights on the system itself. Nevertheless, transient stability analysis constitutes a field that appear particularly interesting for the application of PINNs.

#### A. Test case - network

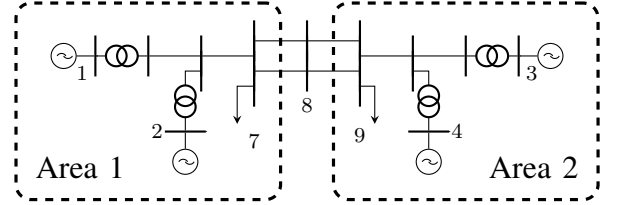


Figure 2. Kundur 2 area system

We study a two-area system adopted from Kundur [13] (refer to page 813 for parameters and a detailed description) as shown in Fig. 2 to investigate the interaction between two weakly linked areas under a set of disturbances and faults. We apply the Kron-reduction to eliminate buses without a generator or load connected to it, i.e. purely algebraic equations. The following governing equations then describe the dynamics of buses with a generator

$$\dot{\delta}_i = \omega_i - \omega_0 \quad (17)$$

$$\dot{\omega}_i = \frac{\omega_0}{2H_i} \left( P_i^{set} + \Delta P_i - \sum_j \frac{V_i V_j}{X_{ij}} \sin(\delta_i - \delta_j) \right) \quad (18)$$

and a load respectively

$$\dot{\delta}_i = \frac{1}{D_i} \left( P_i^{set} + \Delta P_i - \sum_j \frac{V_i V_j}{X_{ij}} \sin(\delta_i - \delta_j) \right) \quad (19)$$

where the rotor angles  $\delta_i$  and the rotor frequencies  $\omega_i$  constitute the states  $\mathbf{x}$  of the system. We fix the bus voltages  $V_i$  to the values obtained from evaluating an AC-power flow using the fixed power set points  $P_i^{set}$ . Besides, we have the inertia and damping constants  $H_i$  and  $D_i$ , as well as the line reactances  $X_{ij}$ . Lastly, the power disturbance  $\Delta P_i$  is the control signal  $u$ , which equals 0 unless stated otherwise. We now apply the following events: 1) a loss of load at bus 7  $\Delta P_7 \in [0.0, 6.0] \text{ pu}$ ; 2) after five seconds (system settled): short circuit at bus 9, i.e.  $V_9 = 0 \text{ pu}$ . 3) after 50 ms: clearing of the short circuit by tripping one line between bus 8 and bus 9, i.e.  $X_{8,9}^{new} = 2 \cdot X_{8,9}^{old}$ . We approximate the evolution after the line trip both with the presented PINNs and compare it to simple NNs and dtNNs. Figure 3 illustrates the resulting dynamics for an exemplary disturbance of  $\Delta P_7 = 2 \text{ pu}$ .

#### B. NN architecture and training setup

We use the machine learning platform TensorFlow [14] for the implementation of the NNs and the training process utilises

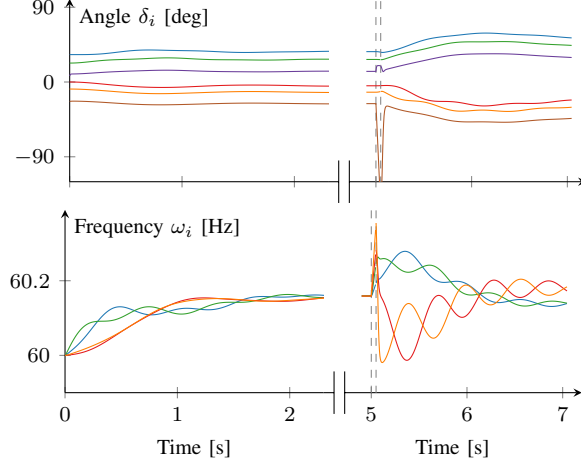


Figure 3. Exemplary power system response under a load disturbance  $\Delta P_7 = 2\text{pu}$  which settled after 5s. This is followed by a short circuit at bus 9 lasting 50ms and the tripping of a line between bus 8 and 9.

the Adam-Optimiser [15] with a decaying learning rate<sup>1</sup>. For all variants of the NNs we use two hidden layers and 150 nodes per layer. The training data are selected from a simulated database which segments the input domain [time and power disturbance] into a equally spaced grid with a 0.001s and 0.002 p.u. granularity. The exact training dataset used in the results section will be specified by the number of trajectories  $N_{traj}$ , i.e. each trajectory links to a power disturbance, and the number of data points along each trajectory  $N_{TS}$ , hence the total number of data points  $N_x = N_{traj} \cdot N_{TS}$ . The collocation points for PINNs form an equally spaced grid with 25 trajectories and 41 instances along each trajectory. We test all types of NN on the entire simulated database, i.e.  $N_{traj} = 301$ ,  $N_{TS} = 2001$ . The reason for not using a validation dataset is that this work does not aim for comparing how well each NN type can be tuned with respect to its hyper-parameters. Instead we opted for choosing hyper-parameters, e.g. the loss term weights, that robustly yield a fair comparison so that we can explore the characteristic of each methodology. For a regular use case the partitioning into a validation and test dataset is strongly encouraged. The data creation and training is all performed on a regular machine (i5-7200U CPU @ 2.50GHz, 16GB RAM).

#### IV. RESULTS

To judge the performance of PINNs we first compare them with a classical numerical solver with respect to their solution time. In a second step we show that PINNs are desireable over classical NN and dtNN in terms of the achievable accuracy for a given dataset. We proceed by providing further insights into the reasons and the consequences for the training procedure.

##### A. Performance of PINNs and classical numerical solvers

The primary motivation to use forms of NNs, here PINNs, for analysing transient stability behaviour is the speed of

<sup>1</sup>Please refer to the published code for details. The initial learning rate is set to values between 0.01 and 0.001 and the decay leads to reduction between one and two orders of magnitude at the end of the training

evaluation. Figure 4a presents a direct comparison of the evaluation time of PINNs and a classical RK45-solver for various time instances across the input domain. While the advantage of PINN ranges on the order of factor 50 for small time steps, the gap increases up to nearly 1000 at  $t = 2\text{s}$ . In Fig. 4b we consider the share of trajectories (in the test dataset) that exhibit an angle difference between bus 7 and bus 9 larger than  $\frac{\pi}{2}$ . For  $t > 0.2\text{s}$  the transmission capacity between the two areas is sometimes not sufficient, hence unstable behaviour can occur. Therefore, a time domain simulation needs to be run until  $t = 1.0\text{s}$ . For this region of interest, the computational advantage is between two and three orders of magnitude, which in turn can allow a denser screening of the cases.

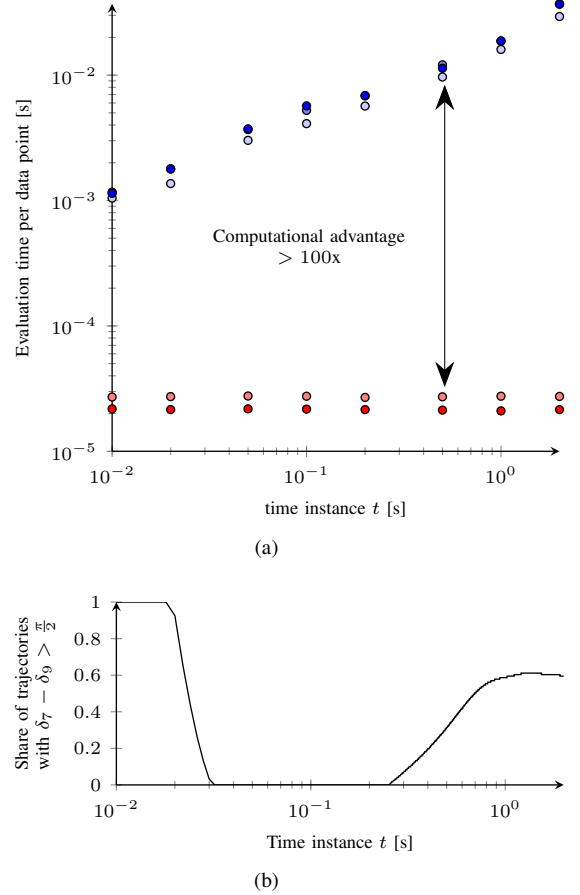


Figure 4. (a) Comparison of the evaluation time of PINNs (red) and an RK45 solver (blue) with different levels of accuracy and size of the NN. (b) critical time to simulate ( $> 0.2\text{s}$ ) where the first trajectories experience unstable system dynamics.

The reason for this behaviour lies in the fact that PINNs require only a single pass through the network and the output trajectory is fully parametrised by the queried time instance. In contrast, the numerical integrator needs successive passes and the number depends on an appropriately chosen step size. A substantial part of the computational expense lies in the initial steps that are governed by a larger non-linearity.

From a complexity analysis perspective, the evaluation time depends solely on the size of the NN, i.e. the number of layers and the number of neurons per layer. Figure 4a shows the effects of a wider network, i.e. more neurons per layer, and a deeper network, i.e. more layers. These parameters determine

the model complexity which is closely linked to how complex the approximated functions can be. The required complexity depends on the input domain and the number of states in the power system as the solution may live on a lower-dimensional manifold which the NN can exploit. Determining how ‘large’ a NN needs to be as a function of the number of states is non-trivial. In contrast, the computational complexity of ODE solvers links directly to the number of states in the system due to the evaluation of (1). For stiff systems the need for implicit solvers and matrix inversion aggravate this. Furthermore, the tolerance of the ODE solver affects the solution time as shown with the blue dots in Fig. 4a, whereas for PINNs the level of accuracy is governed by the training process and not variable during evaluation.

Lastly, the PINN needs to be called only a single time, no matter how many points, because all data points can be evaluated at the same time. The required overhead can thereby be distributed across all data points.

The results as presented hold for all three forms of NN, i.e. classical NNs, dtNNs, and PINNs, because the evaluation of  $\hat{x}$  as shown in Fig. 1 is equal. However, they differ in the training process which governs the accuracy as presented in the subsequent sections.

### B. Accuracy

As we have established the advantage of methods based on NNs over classical solver in terms of evaluation speed, we need to consider how to achieve a required accuracy across the input domain for NN-based methods. Subsequently, the focus lies on the comparison of PINNs with classical NNs and dtNNs with respect to the achievable accuracy and the underlying principles. Therefore, we ask: ‘What level of accuracy can we achieve with a given dataset with each method?’ Figure 5 provides the answer for a number of datasets. These datasets vary in the number of *trajectories*  $N_P$  they contain and the number of data points per *trajectory*  $N_T$ .

The main insight of Fig. 5 is that PINNs consistently outperform simple NNs and dtNNs across all variables and the tested numbers of data points when a limited number of data points is available. To give a benchmark, the blue strip indicates the inter-quartile range of the approximation error of a simple NN trained with a large dataset ( $N_{traj} = 25, N_{TS} = 41$ ). The tested PINNs can even then yield comparably accurate results. Furthermore, the comparison of dtNNs and PINNs underlines the fundamental importance of the collocation points and that PINNs are more than simply evaluating physics at ‘normal’ data points. Only the evaluation of  $\mathcal{L}_f^i$  at the collocation points allows to improve  $\hat{x}$  for a given limited dataset. Beyond this observation, Fig. 5 furthermore show that changing the number of trajectories  $N_{traj}$  or the number of data points per trajectory  $N_{TS}$  have different effects. For more trajectories, the approximation error reduces, in particular for dtNNs, whereas only using more data points per trajectory leads to insignificant accuracy improvements. This effect occurs due to the underlying system of differential equations, as points on a given trajectory are governed by temporal derivatives hence they are linked to each other. Meanwhile, different trajectories

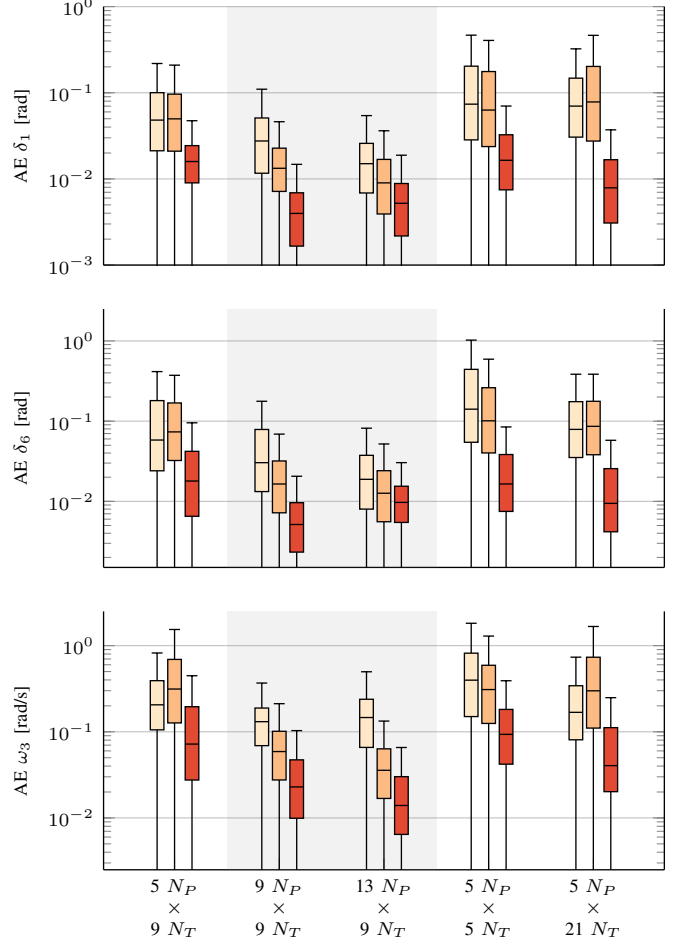


Figure 5. Variation of the absolute error on the test set for different number of trajectories  $N_{traj}$  and points per trajectory  $N_{TS}$  and neural network types. Colours: yellow = NN, orange = dtNN, red = PINN

are not directly linked to each other apart from the underlying equations which leaves the interpolation between trajectories entirely up to the NN. Due to this fundamental difference of the data points, or more precisely due to their marginal information contribution, using physics on data points improves the accuracy only if it can add marginal information beyond the one provided by the additional data points. In case of more data points per trajectory, the contribution of the data points and the physics overlap and therefore we see no significant improvement in the approximation accuracy. However, for more trajectories using physics provides a clear benefit over a simple NN. This is particularly true for the four frequency states  $\omega_1 - \omega_4$ , as they undergo some oscillation that the simple NN cannot capture well.

### C. Interpolation control

To illustrate the added value of additional data points and collocation points (for PINNs) we consider in Fig. 6 a section from the two-dimensional input space, namely in time  $t$  and the power disturbance at bus 7  $\Delta P_7$ . The black dots mark the data points we use for a simple NN and the coloured circles show the used data points in case of more data points

per trajectory (red) and more trajectories (blue). Lastly, the grey dots indicate the collocation points we use for the PINN together with the black dots. The vertical dashed lines represent ‘cross-sections’ along a trajectory. The two upper plots show these trajectories for  $\delta_3$  where the left plot (A) lies on a trajectory with data points while the right one (B) does not, hence is fully subject to the NN’s interpolation. We observe that a NN with more time steps (green dotted line) fits the true trajectory better when looking at the left plots, however, the right plots shows a less accurate prediction. Similarly, the dtNN (orange line) shows some mismatches in the right plots. In contrast a NN with more trajectories (green dashed line) and PINNs (red line) provide better approximations in both cases. Similarly, we can consider specific time instances, the horizontal dashed lines in Fig. 6. These ‘snapshots’ shown in the plots pronounce the value of more trajectories vs more data points per trajectory even more, as the other NNs apart from PINNs show large errors in their interpolation.

#### D. Computation time

Looking from a general perspective, the total computation time to train a NN, dtNN, or PINN consists of three elements: 1) data creation time, 2) training time, 3) evaluation time. The data creation is directly linked to the computational effort associated with using a classical solver as explained in Section IV-A. Section IV-D shows the required time for create the data for the different datasets, the ones with more trajectories require additional time, approximately linearly scaling with  $N_P$  while increasing the number points on a trajectory, i.e.  $N_T$ , barely affects the data generation time. Furthermore, the orange and red bars indicate the additional effort required for dtNNs and PINNs. These are negligible as they are a simple evaluation of  $f$  (for dtNNs) and a sampling of the collocation points.

The second component of the overall computation time concerns the training process. Figure 8 shows the evolution of the loss on the validation dataset which serves as a check when the model begins to overfit. Until epoch 200 all three types quickly reduce the loss, however, afterwards only the PINNs can improve the performance on the validation set. Hence, continuing the training process leads to improved accuracy at the expense of longer computation time. It should be furthermore noted that each epoch of the PINN is associated with a four times larger training time per epoch (from about 55ms to 220ms) due to the necessary evaluation of the collocation points.

The third component of the overall computing time is the evaluation and testing of the model. These are crucial to quantify the level of accuracy that can be achieved. The evaluation itself is cheap apart from the necessary data points as we face the same challenges as in the data creation for the training. This entails that an extensive testing of the model to ensure accurate predictions can be expensive. PINNs do not fundamentally change this problem, however, the evaluation of the physics loss, which does not require the simulation of a single trajectory, might be helpful in reducing the computation burden of the testing effort.

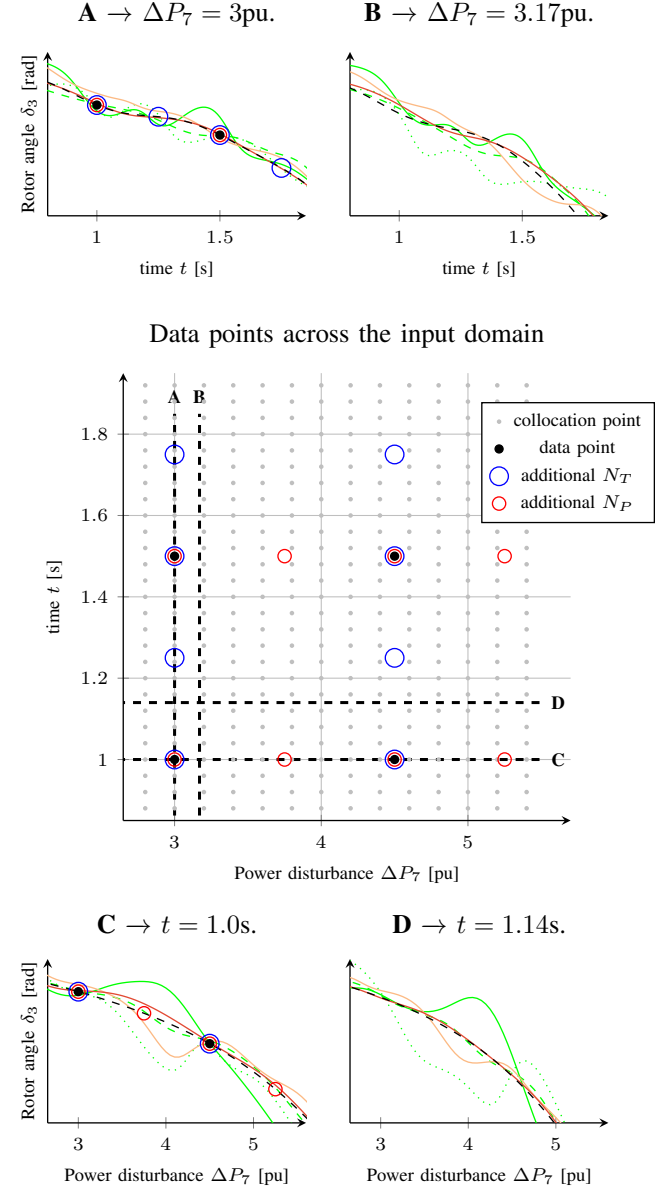


Figure 6. Different number and types of data points and their effect on the interpolation problem across the time and power disturbance domain. Colours: green = simple NN, green dashed = simple NN with more trajectories, green dotted = simple NN with more points per trajectory, orange = dtNN, red = PINN

## V. OPPORTUNITIES AND CHALLENGES OF AND FOR PINNS

With the previous section we have been investigating a very specific case in depth, let us now take a broader view on this method and directions for future work. The most pressing question is indisputably: Does it scale - and what happens when we apply PINNs to larger systems and higher dimensions in the input domain? Given the much-cited ‘Curse of dimensionality’, the latter aspect of scale poses the bigger challenge. However, data creation suffers as well from high dimensionality, and if PINNs can exploit the ‘Blessing of Dimensionality’, they could become more competitive with respect to the combined required time for data creation and training. This leads to two major directions of research, one

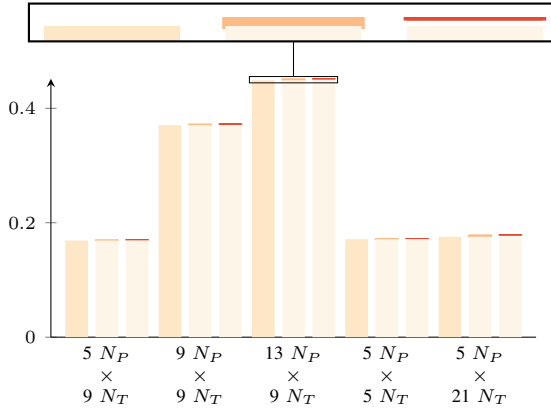


Figure 7. Required computational time for data creation.

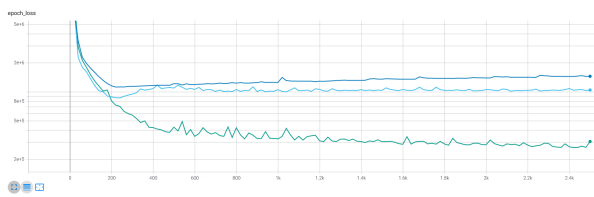


Figure 8. Evolution of the validation loss of NN (dark blue), dtNN (light blue), PINN (green) for  $\hat{x} - x$

more ML oriented and the other more modelling related. From a purely ML perspective there is a vast number of more advanced ML techniques to be explored and tested to make the learning more efficient and faster. This could include NN architectures, training algorithms, parameter initialisations, ... . From a more modelling oriented perspective one can ask how the representation of the physical equations affects the training procedure. An example could be to investigate the effects of a Kron-reduced vs. not-Kron-reduced power system representation. Including higher-order dynamics in the physics regularisation also points into the direction of how the loss  $L_c$  changes the optimisation landscape. Insights from these analyses could help to derive hyper-parameters such as the loss terms weights  $\lambda$ , hence, use as much of the physical models as possible.

A broader line of thought we see, is to try to integrate the aspects of data creation, PINN training, and verification better with each other. Such approaches could use the evaluation of  $\mathcal{L}_c$  to infer the true approximation errors and then either use them for resampling or to provide metrics on the NN's accuracy. In particular, data efficient sampling processes that identify regions in the input domain of higher interest or importance could lead to significant improvements of the entire process.

Borrowing an idea from the ML community, transfer learning could be a direction for PINNs. Transfer learning means that a learning task starts from a model that was trained on a (slightly) different task beforehand. What if we trained a PINN on an intact system under various load disturbances and then change topology by simply adapting the physical equations. Could the new NN profit from the previous network's training?

## VI. CONCLUSION

Approaches to utilise machine learning and neural networks in power systems offer enormous upsides, using their fast evaluation for screening critical operating points or exploiting the their ability to capturing complex phenomena. However, there are significant barriers for adopting ML techniques in power systems - no doubt. Two major barriers are the creation of adequate databases and verifying that the trained neural networks are sufficiently accurate. With PINNs we obtain a new angle to tackle these issues by shifting part of the focus on the learning procedure which then can adopt advanced methods from ML research. This may allow to address some aspect that currently hinder the adoption of ML in adoption and thereby remove the sole reliance on progress on data creation and verification techniques. Furthermore, PINNs link the three topics - data creation, training, verification - together such that synergy effects of more holistic methods could become game changers.

## REFERENCES

- [1] Y. Zhang, L. Wehenkel, P. Rousseaux, and M. Pavella, "SIME: A hybrid approach to fast transient stability assessment and contingency selection," *International Journal of Electrical Power & Energy Systems*, vol. 19, no. 3, pp. 195–208, Mar. 1997. [Online]. Available: <https://linkinghub.elsevier.com/retrieve/pii/S0142061596000476>
- [2] G. Gless, "Direct Method of Liapunov Applied to Transient Power System Stability," *IEEE Transactions on Power Apparatus and Systems*, vol. PAS-85, no. 2, pp. 159–168, Feb. 1966. [Online]. Available: <http://ieeexplore.ieee.org/document/4073002/>
- [3] A. El-abiad and K. Nagappan, "Transient Stability Regions of Multimachine Power Systems," *IEEE Transactions on Power Apparatus and Systems*, vol. PAS-85, no. 2, pp. 169–179, Feb. 1966. [Online]. Available: <http://ieeexplore.ieee.org/document/4073003/>
- [4] L. Duchesne, E. Karangelos, and L. Wehenkel, "Recent Developments in Machine Learning for Energy Systems Reliability Management," *Proceedings of the IEEE*, vol. 108, no. 9, pp. 1656–1676, Sep. 2020. [Online]. Available: <https://ieeexplore.ieee.org/document/9091534/>
- [5] F. Thams, A. Venzke, R. Eriksson, and S. Chatzivasileiadis, "Efficient Database Generation for Data-Driven Security Assessment of Power Systems," *IEEE Transactions on Power Systems*, vol. 35, no. 1, pp. 30–41, Jan. 2020. [Online]. Available: <https://ieeexplore.ieee.org/document/8600355/>
- [6] M. O. Raissi, P. O. Perdikaris, and G. E. Karniadakis, "Physics-informed neural networks: A deep learning framework for solving forward and inverse problems involving nonlinear partial differential equations," *Journal of Computational Physics*, vol. 378, no. C, Nov. 2018, institution: Univ. of Pennsylvania, Philadelphia, PA (United States) Publisher: Elsevier.
- [7] G. S. Misirlis, A. Venzke, and S. Chatzivasileiadis, "Physics-Informed Neural Networks for Power Systems," in *2020 IEEE Power & Energy Society General Meeting (PESGM)*. Montreal, QC, Canada: IEEE, Aug. 2020, pp. 1–5. [Online]. Available: <https://ieeexplore.ieee.org/document/9282004/>
- [8] B. Stott, "Power system dynamic response calculations," *Proceedings of the IEEE*, vol. 67, no. 2, pp. 219–241, Feb. 1979, conference Name: Proceedings of the IEEE.
- [9] G. Cybenko, "Approximation by superpositions of a sigmoidal function," *Mathematics of Control, Signals, and Systems*, vol. 2, no. 4, pp. 303–314, Dec. 1989. [Online]. Available: <http://link.springer.com/10.1007/BF02551274>
- [10] K. Hornik, M. Stinchcombe, and H. White, "Multilayer feedforward networks are universal approximators," *Neural Networks*, vol. 2, no. 5, pp. 359–366, Jan. 1989. [Online]. Available: <https://linkinghub.elsevier.com/retrieve/pii/0893608089900208>
- [11] A. G. Baydin, B. A. Pearlmutter, A. A. Radul, and J. M. Siskind, "Automatic Differentiation in Machine Learning: a Survey," *Journal of Machine Learning Research*, vol. 18, no. 153, pp. 1–43, 2018. [Online]. Available: <http://jmlr.org/papers/v18/17-468.html>

- [12] S. Wang, Y. Teng, and P. Perdikaris, “Understanding and mitigating gradient pathologies in physics-informed neural networks,” *arXiv:2001.04536 [cs, math, stat]*, Jan. 2020, arXiv: 2001.04536 version: 1. [Online]. Available: <http://arxiv.org/abs/2001.04536>
- [13] P. Kundur, N. J. Balu, and M. G. Lauby, *Power system stability and control*, ser. The EPRI power system engineering series. New York: McGraw-Hill, 1994.
- [14] M. Abadi, A. Agarwal, P. Barham, E. Brevdo, Z. Chen, C. Citro, G. S. Corrado, A. Davis, J. Dean, M. Devin, S. Ghemawat, I. Goodfellow, A. Harp, G. Irving, M. Isard, Y. Jia, R. Jozefowicz, L. Kaiser, M. Kudlur, J. Levenberg, D. Mane, R. Monga, S. Moore, D. Murray, C. Olah, M. Schuster, J. Shlens, B. Steiner, I. Sutskever, K. Talwar, P. Tucker, V. Vanhoucke, V. Vasudevan, F. Viegas, O. Vinyals, P. Warden, M. Wattenberg, M. Wicke, Y. Yu, and X. Zheng, “TensorFlow: Large-Scale Machine Learning on Heterogeneous Distributed Systems,” p. 19.
- [15] D. P. Kingma and J. Ba, “Adam: A Method for Stochastic Optimization,” *arXiv:1412.6980 [cs]*, Jan. 2017, arXiv: 1412.6980 version: 9. [Online]. Available: <http://arxiv.org/abs/1412.6980>